

RESEARCH ARTICLE

10.1002/2014JA020958

Key Points:

- Identification of daytime Pi2 at CHAMP depends on frequency of Pi2 oscillation
- Contribution from background frequency can alter low-frequency daytime Pi2s
- Penetration electric fields play major role in the generation of daytime Pi2s

Correspondence to:

N. Thomas,
neethalmariyathomas@gmail.com

Citation:

Thomas, N., G. Vichare, A. K. Sinha, and R. Rawat (2015), Low-latitude Pi2 oscillations observed by polar Low Earth Orbiting satellite, *J. Geophys. Res. Space Physics*, 120, 7838–7856, doi:10.1002/2014JA020958.

Received 22 DEC 2014

Accepted 6 AUG 2015

Accepted article online 10 AUG 2015

Published online 5 SEP 2015

Low-latitude Pi2 oscillations observed by polar Low Earth Orbiting satellite

Neethal Thomas¹, Geeta Vichare¹, A. K. Sinha¹, and Rahul Rawat¹¹Indian Institute of Geomagnetism, Navi Mumbai, India

Abstract Low-latitude Pi2 pulsations in the topside ionosphere are investigated using vector magnetic field measurements from LEO satellite, CHAMP, and underneath ground station. Substorm-associated Pi2s are initially identified using high-resolution data from Indian station Shillong, during 2007–2009, and are further classified into three subgroups of Pi2 band (6–25 mHz), based on its frequency. During nighttime, coherent in-phase oscillations are observed in the compressional component at satellite and horizontal component at underneath ground station for all the Pi2 events, irrespective of the Pi2 frequency. We observe that the identification of daytime Pi2s at CHAMP (compressional component) depends on the frequency of Pi2 oscillation; i.e., 40%, 45%, and 100% of Pi2 events observed in dayside ground station with frequency between 6–10 mHz, 10–15 mHz, and 15–25 mHz were identified at satellite, respectively. At CHAMP during daytime, the presence of a dominant power in the lower frequencies of Pi2 band, which is unique to satellite, is consistently observed and can modify the Pi2 oscillations. Pi2s having frequency >15 mHz are less affected by these background frequencies, and a clear signature of daytime Pi2s at CHAMP is possible to observe, provided that contribution from non-Pi2 frequencies at satellite from the lower end of Pi2 band is eliminated. Daytime Pi2s identified in the topside ionosphere showed coherent but mostly opposite phase oscillations with underneath ground station, and satellite-to-ground amplitude ratio is, in general, found to be less than 1. Present results indicate that a combination of fast cavity-mode oscillations and an instantaneous transmission of Pi2 electric field from high- to low-latitude ionosphere is responsible for the observation of daytime Pi2s.

1. Introduction

The impulsive damped geomagnetic field oscillations in the frequency range 6.6–25 mHz are termed as Pi2 pulsations. These short-lived oscillations are believed to be excited by sources in the nightside magnetosphere. Substorms are identified as one of the common energy sources for Pi2s observed in different regions. During substorm, Pi2s are manifested at ground right from auroral to equatorial latitudes, with different longitudinal extent ranging from midnight sector at high latitudes to several hours of local time including daytime at low latitudes [Keiling and Takahashi, 2011]. Review articles by Olson [1999], Yumoto and CPMN group [2001], and Keiling and Takahashi [2011] discuss different source mechanisms responsible for the generation of Pi2s observed in different latitudes. It is presently understood that high- to middle-latitude Pi2s are associated with the field-aligned currents which are launched in the plasma sheet in association with the disruption of the cross-tail current during substorm onset [Nishimura et al., 2012]. The transverse portion of the disturbances produced at the time of field dipolarization travels via Alfvén modes into the polar ionosphere which in turn is manifested as Pi2 oscillations at these latitudes. On the other hand, the compressional portion of the MHD wave travels earthward across the magnetic field and couples energy to different wave modes [Olson, 1999]. In the inner magnetosphere, these compressional waves excite cavity-like oscillations and are considered as a possible mechanism for low-latitude Pi2s in the nightside.

During substorm onset and expansion phase, Pi2s are often observed in low latitudes over a wide range of longitude and are therefore considered as useful substorm indicators [Sakurai and Saito, 1976; Yumoto, 1986]. Daytime Pi2s are found to be a common phenomenon at low [Sutcliffe and Yumoto, 1989, 1991] and equatorial ground stations [Yanagihara and Shimizu, 1966; Stuart and Barszczus, 1980; Sastry et al., 1983]. In a statistical study by Nose et al. [2006], they have shown that in low latitudes, large-amplitude nighttime Pi2s are often accompanied by daytime ones with similar waveforms. Pi2s observed in day and night ground stations were observed to have nearly identical period and similar phase. However, amplitudes of these oscillations were higher at auroral breakup meridian and decreased with the longitudinal separation from the breakup region. Daytime Pi2s identified near the dip equator are reported to have enhanced amplitudes in comparison to low-latitude ones. Shinohara et al. [1997] attributed it to the instantaneous penetration of

electric field variations from the polar ionosphere to dayside equatorial ionosphere, which amplifies the equatorial currents in the enhanced ionospheric conductivity regions.

Using satellite observations, it is possible to observe Pi2 pulsations at different radial distances from the Earth's surface. In a statistical study of Pi2 properties in the inner magnetosphere ($L < 4$) using Active Magnetospheric Particle Tracer Explorers/Charge Composition Explorer (CCE) satellite and ground observations, *Takahashi et al.* [1995] found that Pi2 oscillations are dominated by compressional and radial components at satellite and are found to have high coherence with H component at low-latitude midnight ground station Kakioka when the satellite was on the nightside. But no convincing evidence of Pi2s was present in CCE observations when the satellite was in the dayside. Nighttime Pi2s are also detected in the topside ionosphere using various LEO satellites. One of the earliest of the nighttime Pi2 reports at ionospheric altitude is by *Takahashi et al.* [1999] using UARS observations. The oscillations are found to be identical and in phase with nightside ground station. Later with the observations using Ørsted [*Han et al.*, 2004] and CHAMP [*Sutcliffe and Lühr*, 2003, 2010] similar Pi2 signatures were identified at ground and satellite, which confirms the existence of Pi2 signatures in the topside ionosphere during nighttime.

Simultaneous occurrence of low-latitude Pi2 oscillations in the night and terminator sides is investigated by *Kim et al.* [2010] using electric and magnetic field measurements from Time History of Events and Macroscale Interactions during Substorms (THEMIS)-E and THEMIS-D satellites located in dawn and dusk sectors, respectively. In this case study, highly coherent oscillations were observed in the poloidal components at satellite in the dawn sector and H at midnight ground station, but at the same time there was no evidence of Pi2s in the dusk sector. The authors suggest that the plasmaspheric resonance energy, which is thought as a possible cause for Pi2s observed in the inner magnetosphere, escapes azimuthally and its longitudinal attenuation is larger on the duskside than on the dawnside. Morning time Pi2s are reported in ETS-VI satellite ($L = 6.3$) observations in the compressional and radial components which showed identical period and waveform with north-south component X at ground [*Nose et al.*, 2003]. The observations are in agreement with cavity oscillations.

Although low-latitude Pi2s are identified at ground in different local time (LT) sectors, its daytime existence in space remains an open debate. *Han et al.* [2004] for the first time reported the identification of low-latitude daytime Pi2s in the topside ionosphere using Ørsted data. They reported 2 day events which showed similar oscillations in satellite compressional and ground H components, having opposite phase and smaller amplitudes at satellite. The authors suggest the source mechanism for the daytime Pi2 to be the currents in the equatorial and low-latitude ionosphere generated by the penetrated electric field impressed in the polar ionosphere during substorm. But other than these 2 day events presented, *Han et al.* [2004] could not identify similar observations of daytime Pi2s. Later *Sutcliffe and Lühr* [2010] using CHAMP data reported that no Pi2 signatures can be detected in topside ionosphere during daytime. They supported their observation with the help of a model adopted from *Kikuchi and Araki* [1979]. According to the model, the electric field imprinted in the polar ionosphere is distributed globally in the Earth-ionosphere waveguide, where the ionospheric electric fields will be mapped upward along geomagnetic field lines, while the magnetic field due to the ionospheric current is confined between the ionosphere and Earth. Hence, toroidal currents flowing on the dayside between ionosphere and ground generate magnetic fields that are confined to the Earth-ionosphere cavity. As a consequence, no Pi2-related magnetic signals can be detected in the topside ionosphere.

Thus, there are two contradicting results about daytime Pi2s above the ionosphere using Ørsted and CHAMP. In this study, we focus on the observational aspect of low-latitude daytime Pi2 oscillations at topside ionosphere using CHAMP along with underneath ground and examine whether daytime Pi2s identified at ground are manifested simultaneously in the topside ionosphere or not.

The paper is organized as follows. In section 2 we discuss the method of Pi2 detection and data set used. Section 3 presents typical examples of Pi2s of different frequencies observed during daytime and nighttime separately. Section 4 discusses the non-Pi2 contribution at satellite. Sections 5 and 6 include discussion and summary, respectively.

2. Methodology and Data

First, the identification of Pi2 events is done using high-resolution and high-precision data from induction coil magnetometer located at ground station, Shillong (SHL; 25.92°N, 91.88°E), India. The data are sampled at

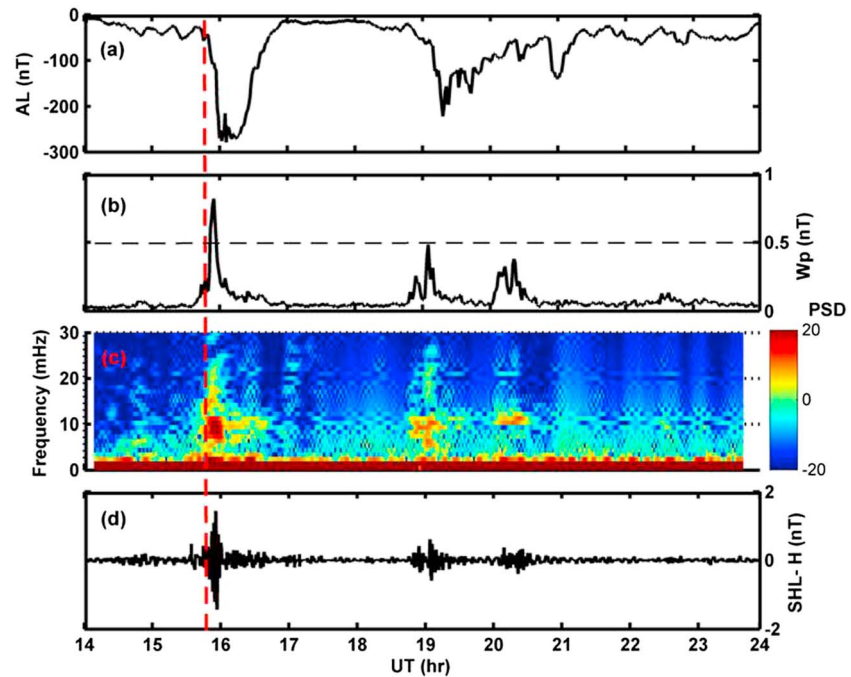


Figure 1. Criteria used for the identification of substorm-associated Pi2 at Shillong (SHL) during nighttime, occurred on 10 February 2007. (a) AL index, (b) W_p index, (c) dynamic spectrum for SHL H , and (d) time series of SHL H component (high pass filtered > 2 mHz). Pi2 onset at 15:48 UT is marked by the vertical red dashed line.

64 Hz with an accuracy of 0.2 pT. Preliminary identification of Pi2 events is done by the visual inspection of the dynamic spectrum and the high-pass-filtered (> 2 mHz) time series of H component at SHL. Spectral plots and the corresponding time series which showed a sudden impulse in the frequency range 6.6–25 mHz are marked as possible Pi2 oscillations. To confirm Pi2 and its association with substorm activity, we further looked into the AL and W_p indices. W_p (Wave and planetary) is a substorm index developed by Nose *et al.* [2012] which reflects the Pi2 power at low latitude. It is considered as a useful indicator of substorm onset. AL and W_p indices together provide the evidence of substorm activity and associated Pi2 oscillations at low latitude. W_p index being sensitive to the onset of even smaller substorms in comparison to AL [Nose *et al.*, 2009], we have chosen W_p (≥ 0.5) as the primary criterion for selecting Pi2 events. AL and W_p values are obtained from World Data Center (WDC), Kyoto, web page. Figure 1 describes the identification of Pi2 event associated with substorm activity. The event presented occurred on 10 February 2007 with Pi2 onset at 15:48 UT. During this event, SHL was in the night sector with LT ~ 22 h. Figures 1a and 1b show the AL and W_p indices respectively for 10 h interval containing Pi2 onset. A sudden depression in AL index by ~ -300 nT and a simultaneous increase in W_p index (~ 0.8 nT) mark the onset of substorm which coincides with Pi2 onset. Figures 1c and 1d show the dynamic spectra and time series respectively of the high-pass-filtered H oscillation at SHL, where a sudden burst having frequency ~ 10 mHz is evident immediately after 15:48 UT. The red dotted line, which marks the onset of Pi2, shows the simultaneous decrease (increase) in AL (W_p), confirming the presence of substorm-associated Pi2s. Other than this event, two more distinct Pi2 impulses at around 19 and 20 UT were clearly seen in the dynamic spectra as well as in the time series. These events are accompanied with simultaneous increase (decrease) in W_p (AL) indices, though W_p is slightly less than 0.5.

Figure 2 describes a typical daytime (near noon) Pi2 event identified at SHL on 23 August 2009. The dynamic spectrum and time series of filtered H component at SHL (Figures 2c and 2d) showed an impulsive oscillation with frequency ~ 14 mHz at 05:14 UT. SHL being in the local daytime, these oscillations are compared with the H variations at a low-latitude station, San Juan (SJG) located near midnight (LT ~ 1 h). The dynamic spectrum (Figure 2e) and high-pass-filtered H oscillations at SJG (Figure 2f) also showed clear Pi2 impulse with onset exactly matching with that at SHL. The onset is marked with red dotted line. The Pi2 impulse observed in

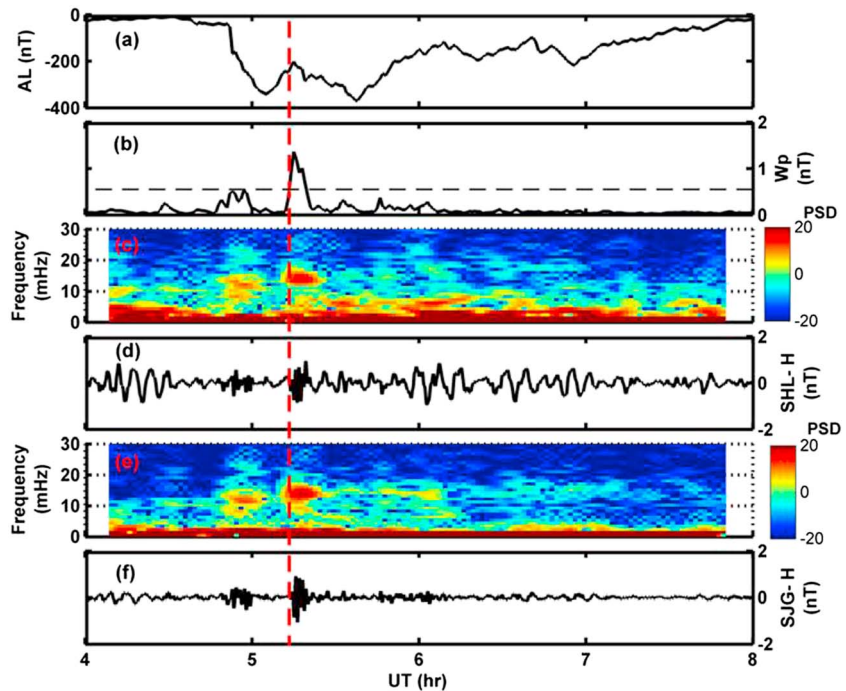


Figure 2. Criteria used for identifying substorm-associated Pi2 at SHL during daytime, on 23 August 2009. (a–d) Same format as in Figure 1. (e) Dynamic spectrum and (f) the time series of H component at midnight station, San Juan (SJG) (high pass filtered > 2 mHz). Vertical red dashed line marks Pi2 onset at 05:14 UT.

SHL as well as SJG H components at 05:14 UT accompanied by a depression in AL by ~ -400 nT and an increase in Wp by ~ 1.5 nT (Figures 2a and 2b) further confirm the existence of substorm-associated Pi2 oscillations. Here one can also note the presence of a Pi2 impulse at $\sim 04:48$ UT in the dynamic spectra (Figures 2c and 2e) and time series (Figures 2d and 2f) of both day and night ground stations with Wp nearing 0.5. Other than these Pi2 oscillations, there are additional undulations present at both ground stations (Figures 2d and 2f), casting their signatures in the dynamic spectra as well (Figures 2c and 2e). The amplitudes of these undulations are higher at dayside station.

Once Pi2s are detected in the ICM data from Shillong observatory as described above, we further look for the location of CHAMP satellite. The present study is limited to the events, for which (1) CHAMP passes were between $\pm 60^\circ$ magnetic latitude; (2) data from underneath low-latitude ground station within $\sim \pm 30^\circ$ of CHAMP longitude are available for the comparison of satellite observations with ground; (3) local time (LT) at CHAMP is either day (07:00–17:00) or night (20:00–04:00); (4) the presence of Pi2 at dayside ground station is ensured before examining daytime Pi2 events at CHAMP; and (5) coherence between satellite and ground oscillations is greater than 0.5 at Pi2 frequency. With the first four conditions we could select a total of 51 Pi2 events with 27 nighttime and 24 daytime events. Consideration of the fifth criteria reduced the number of daytime Pi2 events identified at CHAMP to 12, while the number of nighttime events remained unchanged.

The vector magnetic field measurements in NEC (North East Centre) coordinate with 1 s sampling interval from fluxgate magnetometer on board CHAMP are used for the study. CHAMP (Challenging Minisatellite Payload) was launched in July 2000 into a near-circular polar orbit with an initial inclination of $\sim 87^\circ$ and an altitude of ~ 454 km. The orbital period of CHAMP is around 92 min and therefore makes around 15 day and night passes in 24 h. First, we calculate the residual field at CHAMP by subtracting the main field model POMME 3.1 (Potsdam Magnetic Model of Earth) [Maus and Lühr, 2005] from the observed data. The residual field obtained is then rotated into field-aligned coordinates to get the variations in terms of transverse and longitudinal components. To achieve this, we have adopted the approach discussed by Rajaram *et al.* [1992]. The field-aligned coordinates are defined by the unit vectors $\hat{b}, \hat{\phi} = \hat{b} \times \hat{r} / |\hat{b} \times \hat{r}|$, and $\hat{n} = \hat{\phi} \times \hat{b}$, where $\hat{b} = \vec{B}_0 / |\vec{B}_0|$ is the unit vector along the direction of the background magnetic field \vec{B}_0 at CHAMP. The unit vector \hat{r} is along the radius vector to the

Table 1. List of Ground Stations Used

Ground Stations	Station Code	Geographic		Geomagnetic	
		Latitude (deg)	Longitude (deg)	Latitude (deg)	Longitude (deg)
Shillong	SHL	25.92°N	91.88°E	16.14°N	165.11°E
Kakioka	KAK	36.23°N	140.19°E	27.46°N	150.77°W
Tbilisi	TFS	42.08°N	44.70°E	36.81°N	123.99°E
San Juan	SJG	18.11°N	66.15°W	27.92°N	6.53°E
Stennis	BSL	30.35°N	89.63°W	40.05°N	20.21°W
Honolulu	HON	21.32°N	158.0°W	21.58°N	89.71°W
Ascension Island	ASC	07.95°S	14.38°W	02.52°S	57.06°E

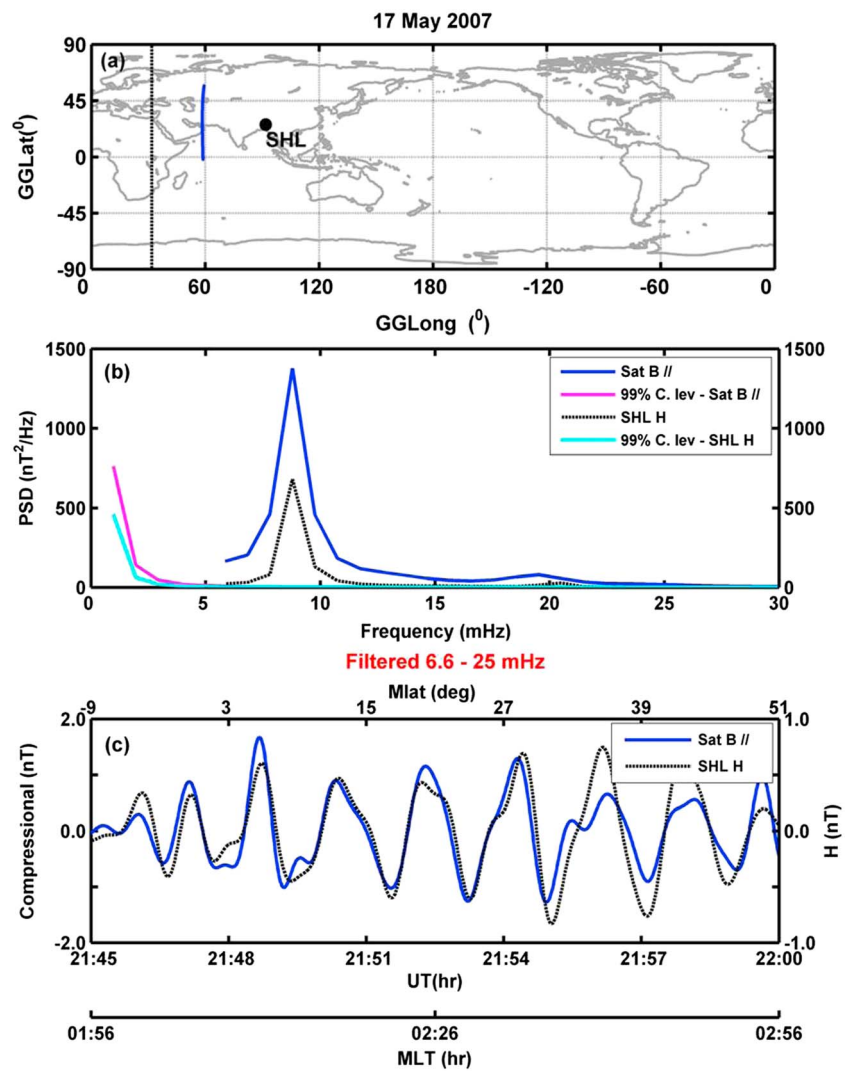


Figure 3. Nighttime Pi2 oscillations (frequency between 6 and 10 mHz) observed on 17 May 2007 when CHAMP and SHL were in nightside. (a) Locations of ground station SHL and CHAMP satellite orbit, with vertical dotted line representing midnight meridian. (b) PSD of CHAMP compressional (Sat B //) and SHL H components. The 99% confidence levels are also shown. (c) Time series of compressional and H components filtered in the frequency range 6.6–25 mHz. Magnetic latitude and the magnetic local time (MLT) values of CHAMP are given at the top and bottom of Figure 3c, respectively. The scale for the satellite component is shown on the left side and that for ground H is shown on the right side for both Figures 3b and 3c.

satellite location. The magnetic field perturbations along the unit vectors \hat{b} , $\hat{\phi}$, and \hat{n} give three orthogonal magnetic field components, namely, compressional (positive northward), toroidal (perpendicular to the field line and azimuthally eastward), and poloidal (perpendicular to the field line and radially inward), respectively. In this study we restrict our analysis to the compressional component observed by the satellite.

Horizontal (H) component of the geomagnetic field from low-latitude ground observatories listed in Table 1 is used in this study. Ground data used from Indian longitudinal sector are induction coil data with 64 Hz sampling recorded at Shillong (SHL) and that from other sectors are fluxgate magnetometer data with 1 Hz sampling. The induction coil data are downsampled to 1 Hz to keep the uniformity in the data set.

3. Observations

Based on the dominant frequency of Pi2 oscillation (defined as characteristic frequency), we classify the identified Pi2s into three different frequency zones viz., 6–10 mHz, 10–15 mHz, and 15–25 mHz. Pi2s observed during nighttime and daytime are presented separately. The LT range of nighttime and daytime has been selected to exclude the terminators, as Pi2 events during terminators can have different properties. Power spectral densities (PSDs) are estimated for satellite compressional and ground H components (band passed between 2 and 25 mHz) using maximum entropy method. PSDs are normalized with respect to the variance of the H oscillations at nightside ground station. A lower cutoff frequency of 2 mHz of the band-pass filter which is well before the lower limit of Pi2 range is used to avoid any modulation of the frequencies of interest.

3.1. Nighttime Pi2 Observations at CHAMP

3.1.1. Pi2 Frequency Between 6 and 10 mHz

Figure 3 describes a nighttime Pi2 event having characteristic frequency between 6 and 10 mHz, occurred on 17 May 2007 with Pi2 onset shortly after 21:45 UT. The event lasted for ~15 min between 21:45 and 22:00 UT. During the event CHAMP and SHL were in the postmidnight sector at ~2 h and 4 h LT, respectively. In this time interval CHAMP was mostly in the Northern Hemisphere moving from approximately 9°S to 51°N. The locations of CHAMP orbit and ground station SHL are shown in Figure 3a. The midnight meridian is marked with vertical dotted line. Figure 3b shows the PSD for CHAMP compressional (blue solid line) and SHL H (black dotted line) components. Identical Pi2 frequency peaks at 9 mHz are observed in both satellite and ground, with higher power at satellite than that at the ground. The 99% confidence levels plotted for satellite compressional (magenta solid line) and ground H (cyan solid line) components confirm that the peaks are well above the confidence level. Figure 3c shows the time series filtered in the conventional Pi2 band (6.6–25 mHz) for satellite compressional (blue solid line) and SHL H (black dotted line) components. Identical in-phase oscillations are evident in both compressional and H components with the higher amplitude at CHAMP than at the ground. The coherence between satellite and ground oscillations is ~1 at Pi2 frequency (9 mHz).

3.1.2. Pi2 Frequency Between 10 and 15 mHz

Nighttime Pi2 event having characteristic frequency between 10 and 15 mHz is presented in Figure 4. The event considered occurred on 13 February 2007 between 15:26 and 15:38 UT with Pi2 onset immediately after 15:26 UT. During the event CHAMP and SHL were in the premidnight sector with LT ~22 h. Dominant Pi2 frequency peak at ~11 mHz (Figure 4b) is evident in both compressional and H components (coherence at 11 mHz is ~1), which are well above the 99% confidence level. The filtered time series (Figure 4c) show coherent in-phase oscillations at satellite and ground with comparable amplitudes.

3.1.3. Pi2 Frequency Between 15 and 25 mHz

Figure 5 shows a nighttime Pi2 event with its characteristic frequency > 15 mHz observed on 2 March 2008. The mean LT at CHAMP and KAK were 22.8 h and 0.4 h, respectively. A clear Pi2 impulse of ~2–3 min duration is evident at ~15:05 UT. Compressional and H components showed identical frequency peak at 15.5 mHz but with slightly higher power at ground than satellite (Figure 5b). High coherence of ~0.9 at Pi2 frequency confirms the simultaneous presence of Pi2 at satellite and ground. Pi2 oscillations at satellite and ground appeared to be matching and in phase with slightly higher amplitude at ground (Figure 5c). Here it can be noted that the ground station is close to the midnight meridian, while satellite was in the premidnight (~23 LT) sector, which might result in the higher Pi2 amplitudes at ground, unlike other nighttime observations presented above.

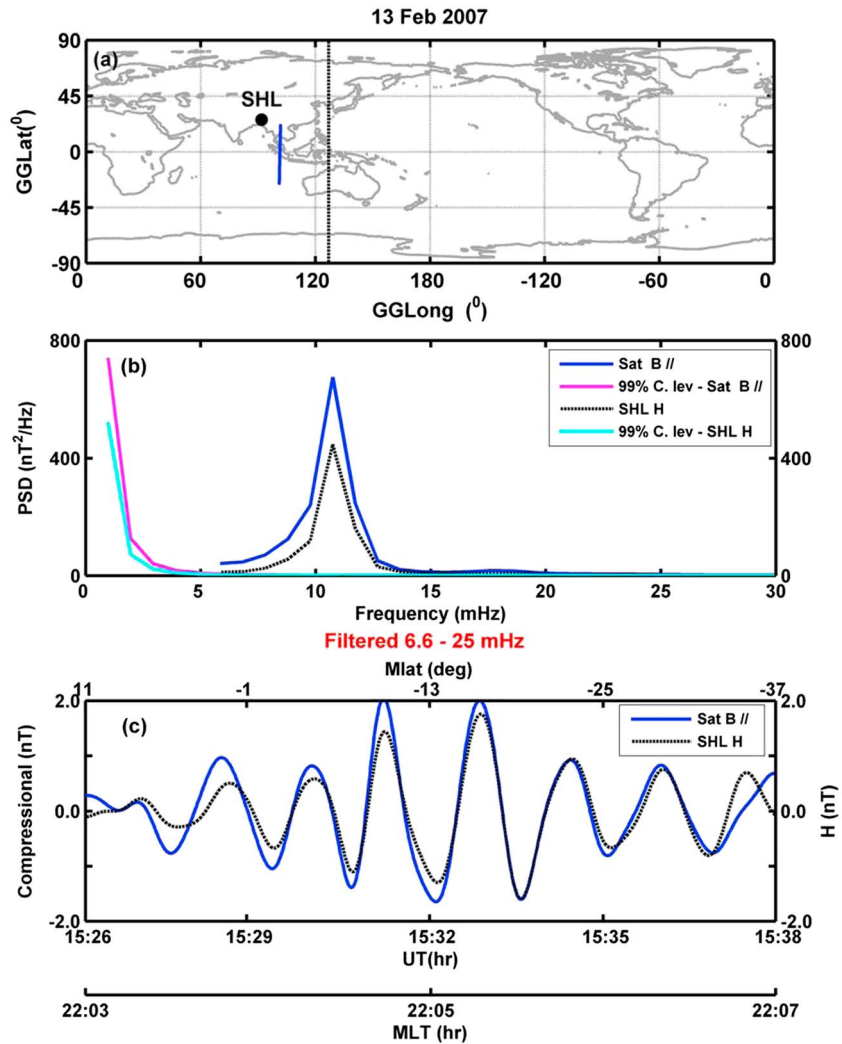


Figure 4. Nighttime event occurred on 13 February 2007 at CHAMP and SHL with Pi2 frequency between 10 and 15 mHz. Format is the same as in Figure 3.

3.1.4. Summary of Nighttime Observations

Apart from the events presented above, we have identified 24 more nighttime cases with different Pi2 frequencies. All 27 nighttime events are filtered in the conventional Pi2 band (6.6–25 mHz), and their wave characteristics are displayed in Figure 6 (shaded area). All nighttime events falling in three different frequency groups (shown by different symbols) showed high coherence (>0.6) (Figure 6a) between satellite compressional and ground H components. The cross-phase angle between satellite and underneath ground oscillations is found to be less than 30° (Figure 6b) for all the nighttime events. Figure 6c shows the percentage of events having satellite to ground amplitude ratio less than 1, where nighttime events are shown by black bars. These percentage values are found to be 25, 8, and 43 in the frequency bands 6–10 mHz, 10–15 mHz, and 15–25 mHz, respectively (average $\sim 25\%$), indicating that $\sim 75\%$ of nighttime events have higher amplitude at satellite. The coherent in-phase oscillations observed in the compressional component at satellite and H at the ground are in accordance with previous satellite-based studies suggesting cavity-mode oscillations during nighttime [Takahashi et al., 1995; Sutcliffe and Lühr, 2003; Sutcliffe and Lühr, 2010; Han et al., 2004; Cuturrufo et al., 2014]. If Pi2 pulsations are generated by the cavity-mode resonance, then those Pi2 signatures should appear in the poloidal component as well [Takahashi et al., 1995; Sutcliffe and Lühr, 2010]. Therefore, in order to confirm the existence of cavity-mode oscillation, we examined the poloidal component at satellite. Around 90% of the nighttime events showed matching oscillations of the same periodicity in the poloidal component with that of the satellite compressional and

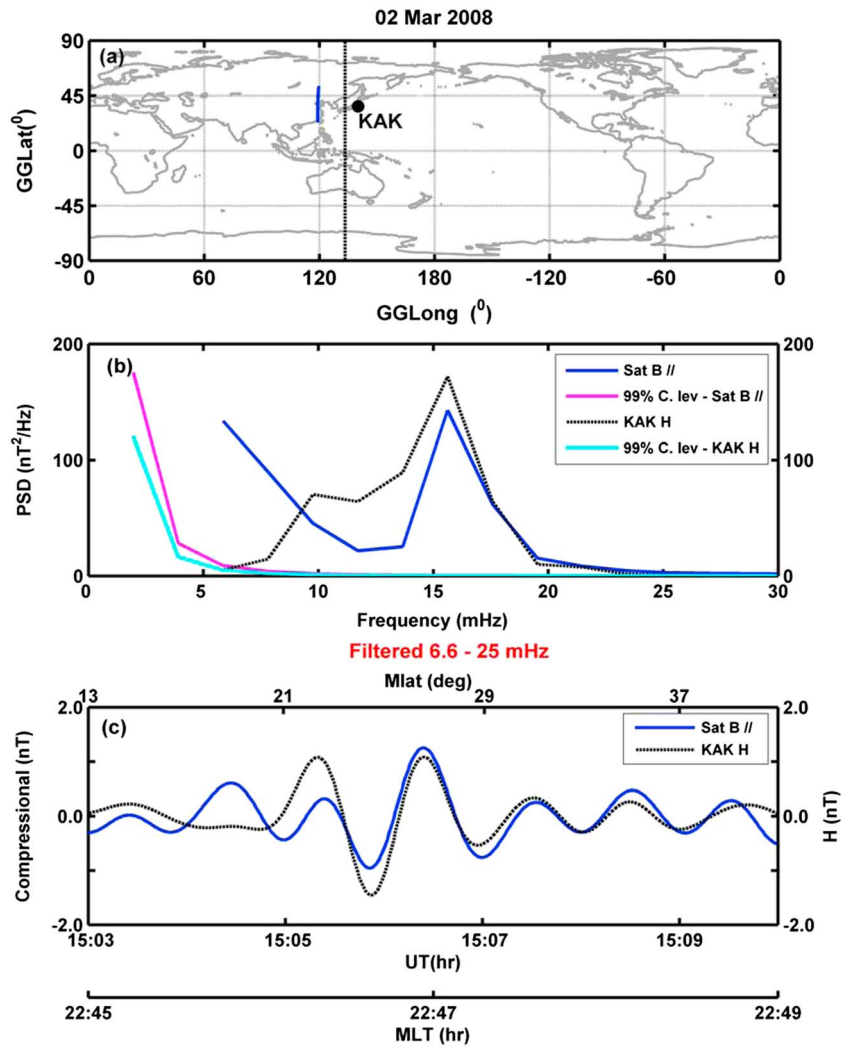


Figure 5. Nighttime Pi2 event observed on 2 March 2008 at CHAMP and KAK with frequency >15 mHz. Format is the same as in Figure 3.

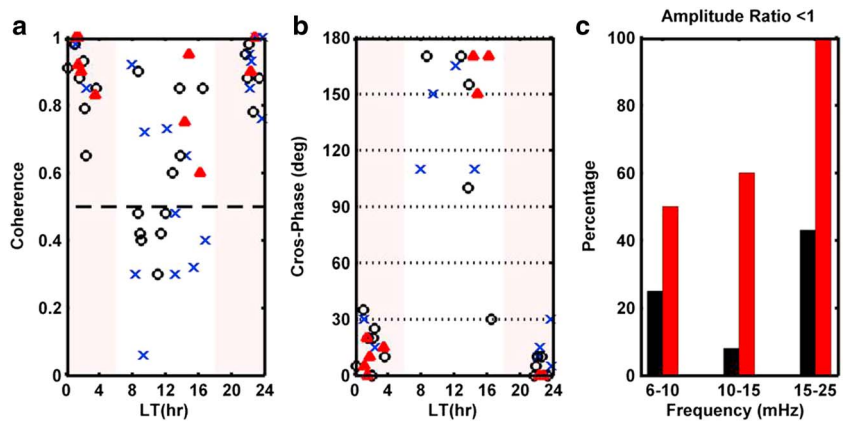


Figure 6. Statistical results of the characteristics of Pi2 oscillations in the frequency bands 5–10 mHz (crosses), 10–15 mHz (circles), and 15–25 mHz (filled triangles). LT dependence of (a) coherence and (b) cross-phase angle between satellite and underneath ground station. (c) Bar plot showing the percentage of events with satellite to ground amplitude ratio less than 1 for day (red bar) and night (black bar) LT. Events with coherence > 0.5 are used in Figures 6b and 6c.

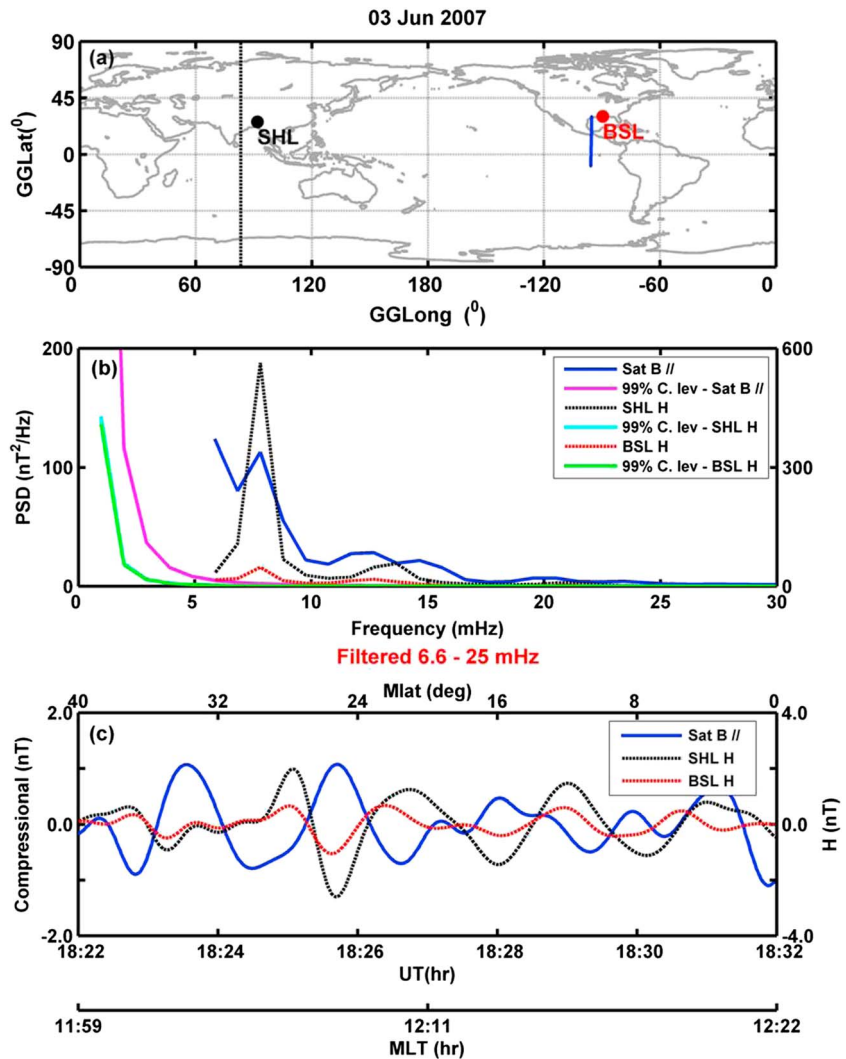


Figure 7. Daytime Pi2 event (frequency <10 mHz) occurred on 3 June 2007 when CHAMP and BSL were in the dayside and SHL was located in the nightside. (a) Locations of SHL, BSL, and CHAMP satellite orbit; midnight meridian is shown by vertical dotted line. (b) PSD of compressional component at CHAMP (Sat B //) and *H* components at SHL and BSL, along with 99% confidence levels. (c) Time series of compressional and *H* components filtered in the frequency range 6.6–25 mHz.

ground *H* components, thereby confirming the cavity-mode resonance as viable generation mechanism for nighttime Pi2 oscillations. We also examined the signature in the toroidal component and found that Pi2 events were absent in the toroidal components for over 60% of nighttime events.

3.2. Daytime Pi2s

In this section we present daytime Pi2 events observed at CHAMP with simultaneous observations from low-latitude ground stations from both day and night sectors.

3.2.1. Pi2 Frequency Between 6 and 10 mHz

Figure 7 shows a noon time Pi2 event having characteristic frequency less than 10 mHz. The event occurred on 3 June 2007, with the Pi2 onset after 18:22 UT. The mean LT at CHAMP, BSL, and SHL were 12.2 h, 12.4 h, and 0.5 h, respectively (Figure 7a). PSD (Figure 7b) shows identical frequency peak at 8 mHz in the midnight ground station SHL (black dotted line) and daytime ground station BSL (red dotted line). Pi2 power is found to be much higher at night ground station compared to day ground station. Although identical peak at 8 mHz is evident in dayside CHAMP observations, contribution from lower frequencies is also observed (blue solid line), which is absent on ground. The wave power of Pi2 frequency at CHAMP is higher than that of underneath ground station BSL. The Pi2 frequency peaks observed at all three locations are well above the

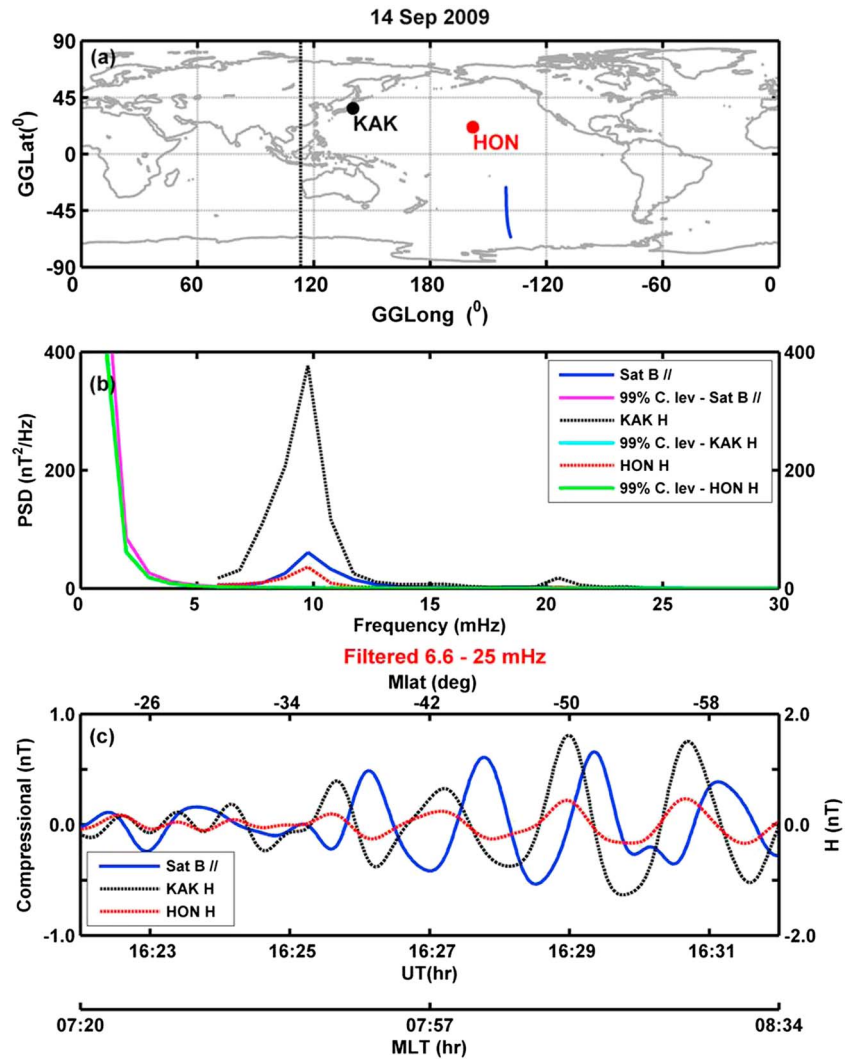


Figure 8. Morning time Pi2 event having frequency <10 mHz observed on 14 September 2009 when CHAMP and HON were located on dayside and KAK was located on nightside. Format is the same as in Figure 7.

confidence level, with very high coherence values (~0.9 between two ground stations and ~0.7 between satellite and dayside ground station). Figure 7c depicts the identical in-phase oscillations in *H* component at SHL and BSL with higher amplitude at nightside station than that at day. A good cross correlation (CC) of 0.8 at nearly zero time lag is observed between two ground stations. Compressional oscillation at CHAMP shows a moderate match with that of *H* at day ground with a maximum CC value of -0.6. Main Pi2 impulse during 18:24–18:27 UT shows opposite phase at satellite and ground with satellite amplitude higher than dayside ground. However, there are additional oscillations with higher amplitude at CHAMP (18:22–18:24 UT), which are not present in the day and night ground observations.

Figure 8 shows a morning time event with Pi2 frequency ≤ 10 mHz, occurred on 14 September 2009 at 16:25 UT. At the time of the event CHAMP and HON were in early morning sector with mean LT ~8 h and 6 h respectively and KAK was in postmidnight sector at ~2 h. Identical frequency peak (Figure 8b) at ~10 mHz is evident in both ground stations, with the daytime Pi2 power much smaller than the nighttime one. Satellite observations also showed exactly identical frequency peak at 10 mHz (coherence ~0.9), with slightly higher power at satellite than daytime ground. Filtered time series in conventional Pi2 frequency band, presented in Figure 8c, showed identical in-phase oscillations at both ground stations (CC ~ 1 at zero lag). Oscillations at satellite are also found to be matching with dayside ground showing a good CC of 0.8 at -30 s lag (which corresponds to nearly

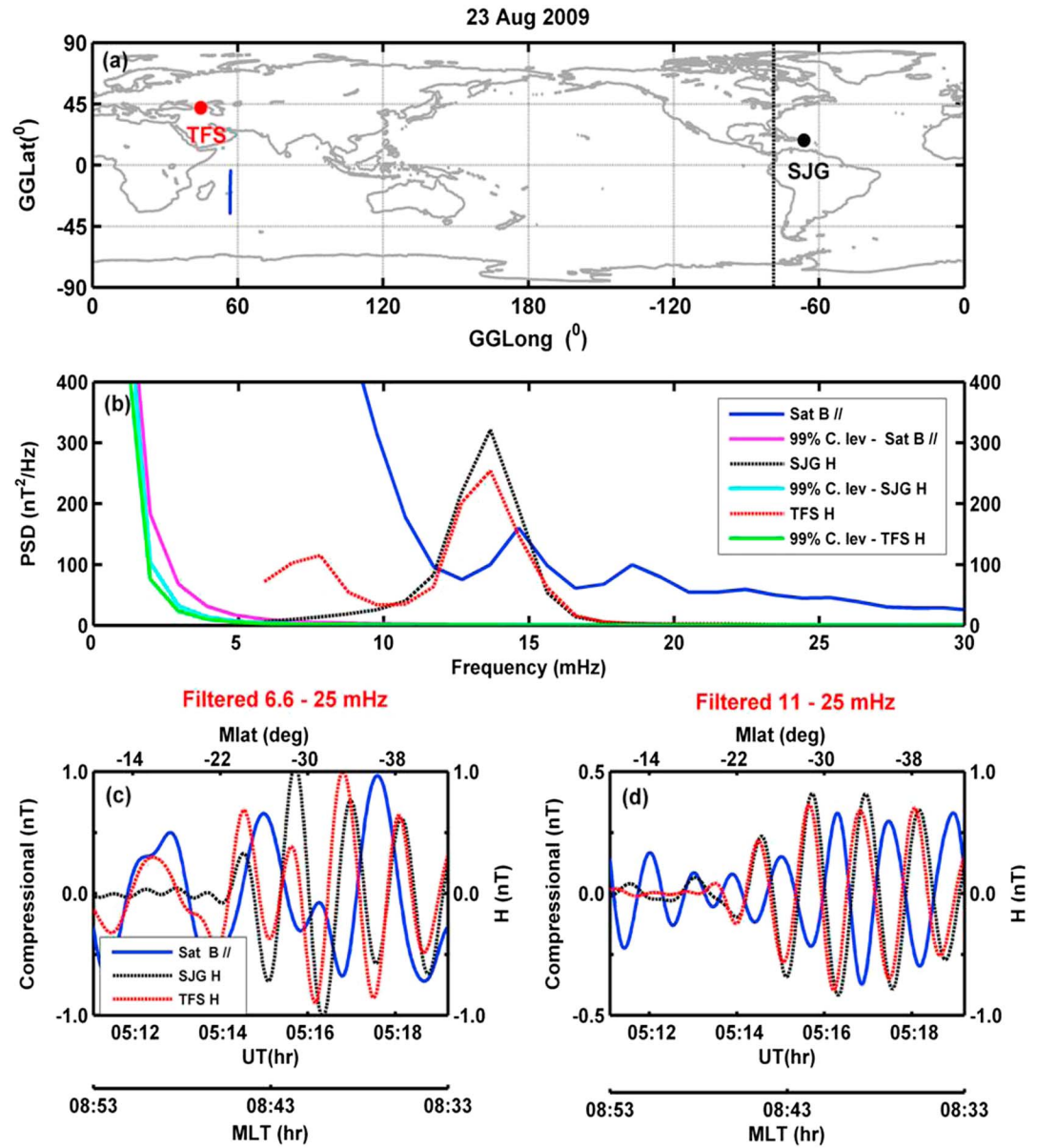


Figure 9. Daytime Pi2 event having frequency between 10 and 15 mHz observed on 23 August 2009, when CHAMP and TFS were in the dayside and SJG was in the nightside. (b and c) Same format as in Figures 7b and 7c. (d) Time series of compressional and *H* components filtered in the frequency band of 11–25 mHz.

100° shift for 10 mHz). Thus, the fluctuations at CHAMP appear to be phase shifted (Figure 8c). Pi2 amplitudes at both CHAMP and HON are observed to be nearly half that of the night station KAK.

3.2.2. Pi2 Frequency Between 10 and 15 mHz

In Figure 9, we present a daytime Pi2, having characteristic frequency between 10 and 15 mHz. The event occurred on 23 August 2009, with the Pi2 onset at ~05:14 UT. The LT at CHAMP, TFS, and SJG were 8.7, 8.1, and 0.7 h, respectively. Both ground stations in the day (TFS) and night (SJG) sectors showed identical frequency peaks at 13.7 mHz, with slightly higher power at SJG than at TFS. Compressional component at satellite showed a shifted frequency peak at ~14.6 mHz (shift is less than 1 mHz). Coherence between satellite and ground at 13.5–15.5 mHz frequency range is found to be near 0.8. Other than this common Pi2 peak near 14 mHz, compressional component at satellite showed a dominant power in the lower frequency band of Pi2, which was not present in night and found to be less dominant in dayside ground station. Figures 9c and 9d show band-pass-filtered time series in the frequency range 6.6–25 mHz (full Pi2 frequency range)

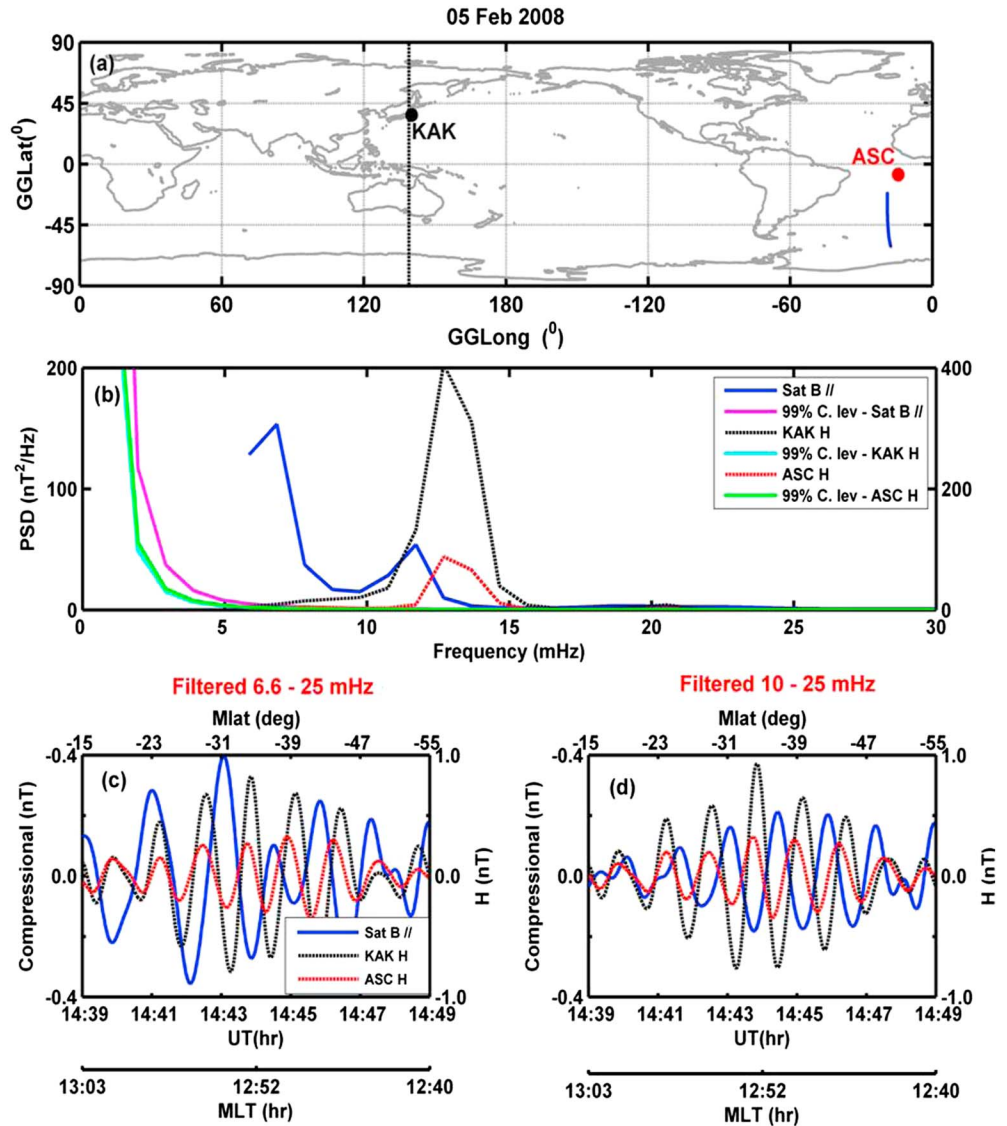


Figure 10. Pi2 event with frequency between 10 and 15 mHz occurred on 5 February 2008 when CHAMP and ASC were in the dayside and KAK was in the nightside. The format is the same as in Figure 9. (d) Narrowband filter applied in the frequency range 10–25 mHz.

and 11–25 mHz (excluding lower frequencies of Pi2 band), respectively. Though there are identical near-in-phase oscillations at two ground stations, the match with the satellite compressional component is poor, when filtered in the conventional band (Figure 9c). The correlation between the oscillations at CHAMP and ground is found to be poor, with maximum CC value of 0.35 at –35 s lag. The dominant power from the lower range of Pi2 band seems to have stronger influence in the oscillations at satellite, leading to poor match with ground Pi2 oscillations. So in order to avoid this non-Pi2 contribution, we filtered the data in a frequency band ranging 11–25 mHz (Figure 9d). A significant increase in CC (–0.7 at time lag nearly 0 s) between satellite and ground is observed with this new band-pass-filtered time series. Thus, the compressional component at satellite oscillates antiphase with ground *H* components. The amplitude of the daytime Pi2 oscillations is observed to be higher at ground compared to CHAMP.

In Figure 10, we present one more case of daytime Pi2, having characteristic frequency between 10 and 15 mHz. The event took place on 5 February 2008, immediately after 14:39 UT. The mean LT at CHAMP, ASC, and KAK were 12.8 h, 13.6 h, and 23.9 h, respectively. Identical Pi2 frequency peak at 12.6 mHz is present in both day (ASC) and night (KAK) ground stations, whereas compressional component at satellite showed a

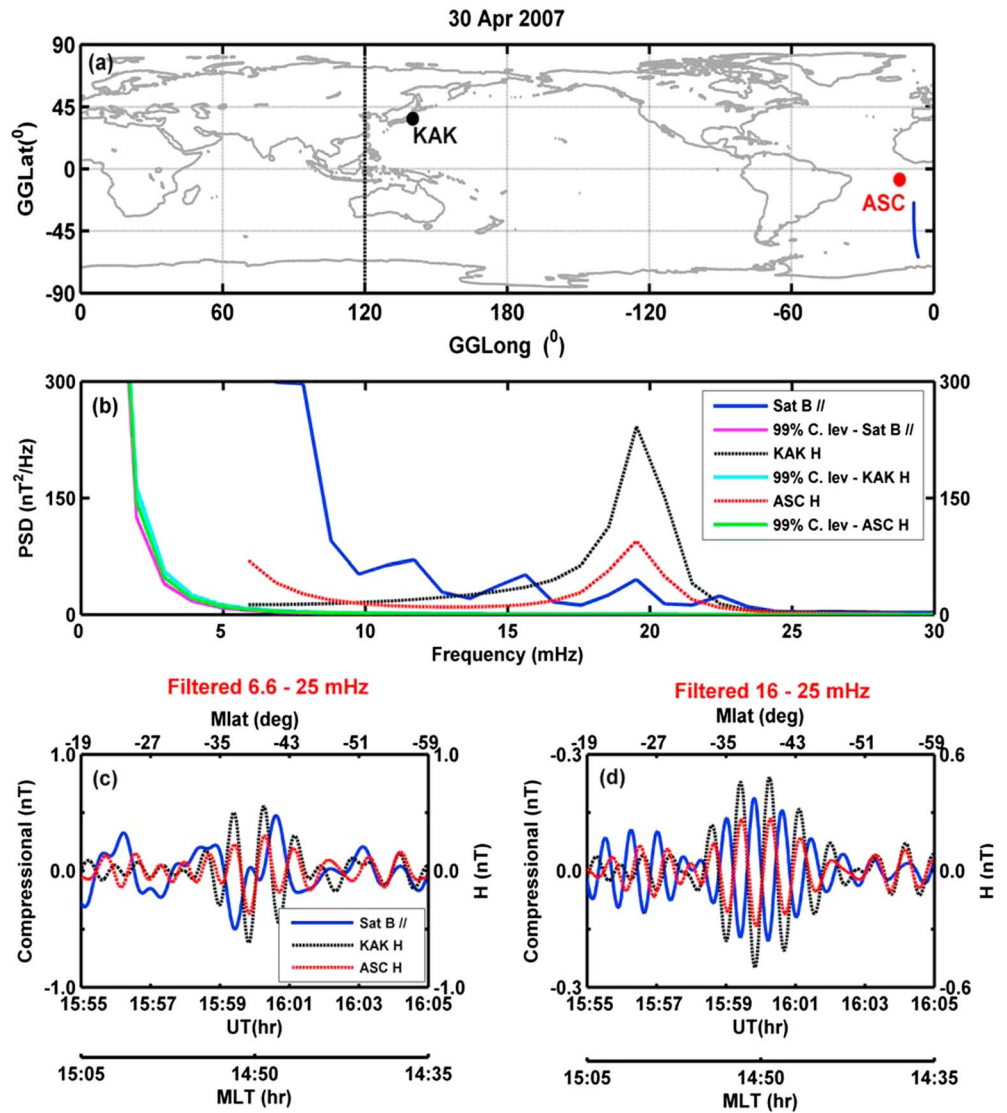


Figure 11. Daytime Pi2 event having frequency >15mHz observed on 30 April 2007 when CHAMP and ASC were in the dayside and KAK was in the nightside. Figure 11 is in the same format as in Figure 9. (d) Time series filtered in the frequency range 16–25 mHz.

slightly shifted (by less than 1 mHz) peak at ~11.7 mHz (coherence ~0.6). Apart from this Pi2 peak (at ~12 mHz), compressional component showed a dominant peak at 7 mHz, which was absent in both ground stations. Similar to the previous event when filtered in the conventional Pi2 range, a poor match between satellite and ground is observed (Figure 10c). The compressional oscillations appear to be modified by the lower frequency component present at CHAMP. To get clear Pi2 oscillations at satellite, this lower frequency component is avoided by filtering in the band 10–25 mHz, which resulted in highly matching oscillations in both satellite and ground (Figure 10d). In the conventional Pi2 band the oscillations at satellite and ground showed a poor CC ~ -0.3 at (-10 s lag) which improved to ~ -0.8 (at -10 s lag) on applying a band-pass filter between 10 and 25 mHz. Therefore, removing the lower frequency contribution within the Pi2 band at satellite brings out the matching signature of Pi2 with that on ground. This treatment helps us in clearly identifying the presence of daytime Pi2 oscillations, which otherwise lead to the belief that Pi2 oscillations do not exist at satellite altitude. Compressional component oscillates nearly antiphase with ground H components, with compressional amplitude smaller than H oscillations at ASC. Also, the amplitude of the Pi2 oscillations is observed to be higher in the night sector compared to that in the day sector (both satellite and ground).

3.2.3. Pi2 Frequency Between 15 and 25 mHz

Figure 11 (same format as of Figure 9) shows a typical daytime Pi2 event with characteristic frequency greater than 15 mHz. The Pi2 event occurred on 30 April 2007 in the interval 15:55–16:05 UT, when CHAMP and ASC were in the dayside with mean LT \sim 14.8 h and KAK was in the postmidnight sector at \sim 1 h. PSD (Figure 11b) shows a dominant peak at 19.5 mHz in the KAK H component, thereby implying that the Pi2 frequency of the considered event resides in the higher side of Pi2 band. H oscillations in the dayside ground station ASC also showed identical frequency peaks, confirming the presence of Pi2 in the dayside ground station. Matching frequency peak is also observed in the compressional oscillations at CHAMP. In addition to the Pi2 frequency peak at 19.5 mHz, compressional component also showed dominant peak in the lower frequency range of Pi2 (at \sim 8 mHz), together with other peaks at 11.8 and 15.5 mHz. Pi2 power is observed to be higher at KAK (nightside) compared to ASC (dayside), and dayside ground is higher than that at satellite. A good coherence of \sim 0.9 is observed between day and night grounds as well as between satellite and ground oscillations at Pi2 frequency around 19–20 mHz. Time series filtered in the frequency ranges 6.6–25 mHz and 16–25 mHz are shown in Figures 11c and 11d, respectively. It is clearly seen from Figure 11c that although day and night ground stations show matching impulsive in-phase oscillations, waveform at satellite is altered. The cross correlation between satellite and ground is found to be 0.35 at a lag of 25 s. In other words we can say that the presence of additional frequencies in the compressional component (which are absent in day and night ground stations) modifies the Pi2 signatures at satellite. In order to avoid these frequencies, we applied a filter in the narrow frequency band 16–25 mHz range, which shows clear Pi2 oscillations at CHAMP matching with ground. The CC between satellite and ground is found to be improved significantly to \sim –0.8 at nearly zero lag on applying this narrowband filter. Dayside Pi2 oscillations observed at satellite are lower in amplitude and opposite in phase compared to ground (ASC) (Figure 11d).

Figure 12 shows another daytime Pi2 event having characteristic frequency $>$ 15 mHz occurred on 22 May 2008. The PSD (Figure 12b) at day (ASC) and night (KAK) ground stations showed identical Pi2 frequency peak at around 15.5 mHz, and a good coherence \sim 0.9 is observed at this frequency. Satellite observations also showed matching Pi2 peak with ground (coherence \sim 0.6 at Pi2 peak); however, a dominant power unique to satellite is obvious in the lower frequency side. Figure 12c shows matching oscillations at both the ground stations (CC \sim 0.9 at zero lag), but the match with the satellite is poor (CC \sim –0.3). As the dominant Pi2 frequency is at \sim 15.5 mHz, we applied a band-pass filter in the frequency range 13–25 mHz in order to avoid the lower frequency part that contaminates the Pi2 oscillations at CHAMP. Figure 12d presents highly correlated (CC \sim –0.95 at nearly zero lag) oscillations at satellite and ground. Pi2 oscillations are found to be antiphase above and below the ionosphere, with the amplitude of oscillations at satellite smaller than that of underneath ground.

3.2.4. Summary of Daytime Observations

Other than the six events presented above, we have identified 18 more daytime Pi2 events that occurred at day and night low-latitude ground stations simultaneously with coherence $>$ 0.8.

Besides the two events presented for Pi2 frequency $<$ 10 mHz, there were two more daytime events from the same frequency group, which showed Pi2 oscillations at both the dayside satellite and the ground. But at the same time, there were six other events for which the simultaneous oscillations were absent at satellite. In those six cases, a strong power in the lower frequency side of Pi2 band was present, which appeared to modify the Pi2 frequency at CHAMP. As a result, we could not identify an isolated well-defined Pi2 frequency peak at satellite, even though it was present in both day and night ground stations. In these cases, the coherence and CC between satellite and ground were found to be poor ($<$ 0.5). The Pi2 events which showed simultaneous oscillations at satellite might have suffered less alternation at CHAMP compared to the other six events. This may be because of either the high intensity of Pi2 event that might have marked its signature despite the presence of lower frequency contribution (Figure 8) or the less dominance of non-Pi2 power at satellite during morning time (Figure 9).

In case of Pi2s with frequency between 10 and 15 mHz, other than the two presented events (both near noon), there were three more daytime Pi2 events observed in CHAMP. But there were six events which were not unambiguously identified at CHAMP. A total of three cases of daytime Pi2s with frequency $>$ 15 mHz were detected at the topside of the ionosphere. In general, we found smaller CC values (–0.3 to –0.35) between satellite and ground oscillations when filtered in the conventional Pi2 band. Application of a band-pass filter that excludes the lower frequencies present at satellite resulted in a significant increase in CC (–0.7 to –0.8) with nearly 180° phase shift between satellite and ground.

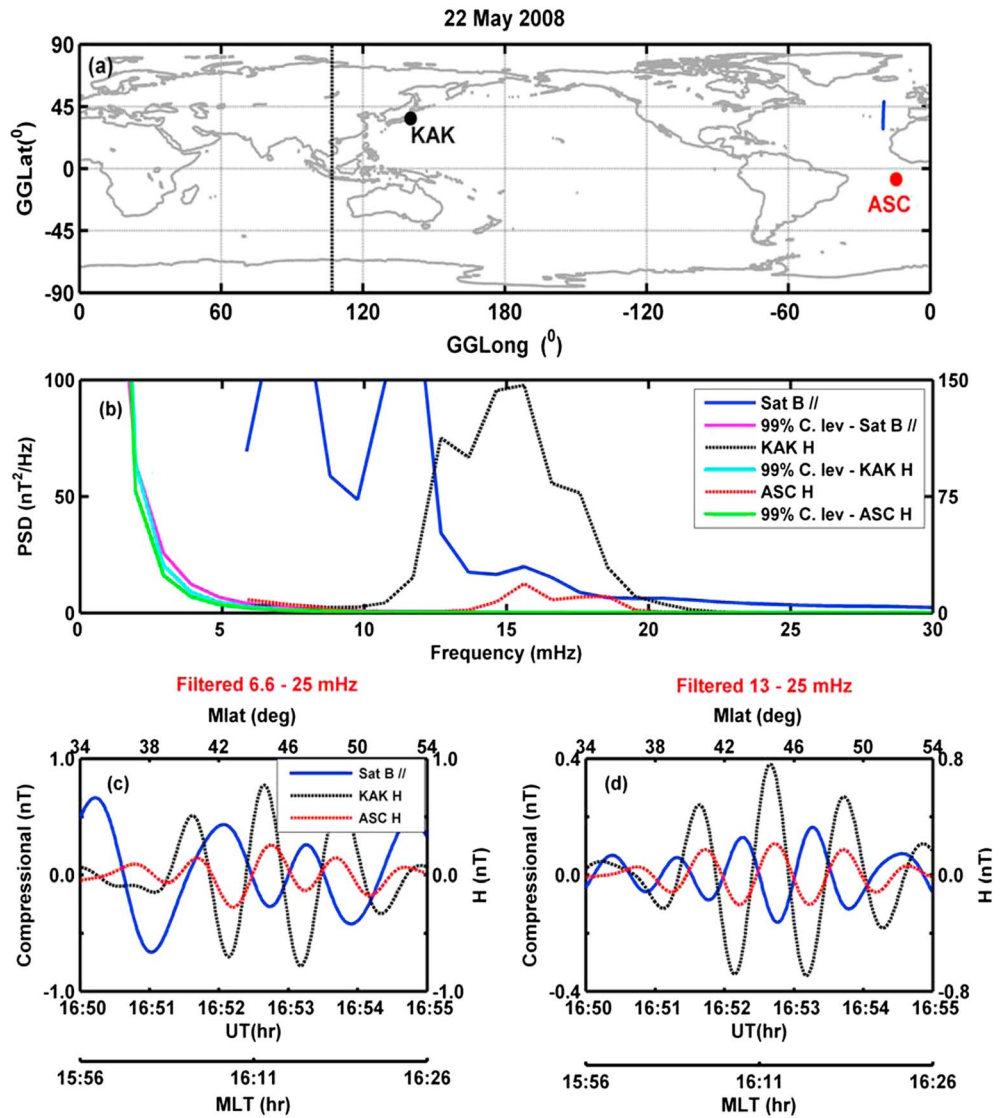


Figure 12. Pi2 event with frequency >15 mHz observed on 22 May 2008 when CHAMP and ASC were in the dayside and KAK was located in the nightside. Format is the same as in Figure 9. (d) Filtered time series in the frequency range 13–25 mHz.

Generally, the amplitude of the Pi2 oscillations on ground is found to be greater than at the satellite resulting in satellite to ground ratio less than 1.

Thus, it is evident from the present investigation that during all daytime events, CHAMP observes a significantly strong power of non-Pi2 origin consistently in the lower frequency range of Pi2 band. These strong lower frequency oscillations can greatly modify the characteristics of temporal oscillations of Pi2s at satellite which have relatively smaller amplitudes. As a result, monitoring Pi2 signatures at CHAMP during daytime will largely depend on its characteristic frequency. The wave characteristics of all Pi2 events summarized in Figure 6 clearly demonstrate this aspect of the daytime Pi2s. Pi2s falling in lower frequency range <10 mHz are found to be more prone to contamination as they are significantly overlapped by lower non-Pi2 frequencies. Figure 6a shows that out of total 10 daytime Pi2 events identified in this range (shown by crosses in Figure 6a), only four events (40%) showed coherent oscillations at satellite (>0.5). In the intermediate frequency range (10–15 mHz) shown by circles, 5 out of 11 cases (45%) showed simultaneous oscillations at satellite. The Pi2 events are observed to be sufficiently intense for those cases for which simultaneous oscillations were detected at satellite. Pi2s falling in the higher frequency end (>15 mHz) (shown by filled

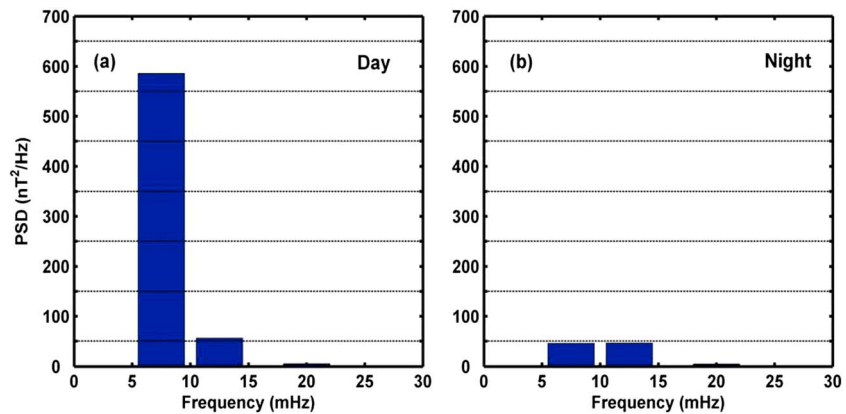


Figure 13. Bar plot showing average power spectral density (PSD) of residual total field for all quiet days with $\sum Kp \leq 5$ of the years 2007–2009 in three frequency bands 5–10 mHz, 10–15 mHz, and 15–25 mHz for (a) day (09:00–17:00 h) and (b) night (21:00–05:00 h) local time sectors.

triangles) are found to be least affected. In this frequency regime we came across only three dayside events and markedly all the three (100%) events were identified concurrently at satellite. Thus, the coherence between satellite and ground oscillations during daytime is found to vary with Pi2 frequency. In general, the coherence is smaller during daytime compared to that during nighttimes.

Other characteristics of Pi2 signatures such as cross-phase angle and amplitude ratio between satellite and ground (Figures 6b and 6c) are computed only for the events with coherence > 0.5 . These events are further narrow band filtered to eliminate the non-Pi2 contribution at the satellite. The cross-phase angles are found to be higher during daytime ($> 90^\circ$) when compared to night. The percentage of events having satellite to ground amplitude ratio less than 1 is found to be 100% for Pi2s with frequencies > 15 mHz. The percentages are 50 and 60 for the frequencies < 10 mHz and 10–15 mHz bands, respectively. This indicates that on average 70% of daytime Pi2 events showed smaller amplitudes at satellite compared to ground. Apart from compressional component, we have also examined the poloidal and toroidal components at satellite. In all the daytime events we could not identify coherent Pi2 signatures in these components.

4. Non-Pi2 Contribution at Satellite

In order to examine the presence of lower frequencies that are present at the satellite, we investigated the frequency spectra of total magnetic field measurements at CHAMP during international geomagnetic quiet days ($\sum Kp \leq 5$) of the years 2007–2009 and estimated the power in different frequency bands: 5–10 mHz, 10–15 mHz, and 15–25 mHz. The maximum power in each frequency band is identified for all day (09:00–17:00) and night (21:00–05:00) satellite passes separately. The averaged PSD estimated from over 1905 (127×15 passes) satellite passes for daytime and nighttime each in the three frequency bands is shown in Figure 13. During daytime, the largest power is observed between 5 and 10 mHz, which decreases significantly in 10–15 mHz and 15–25 mHz bands (Figure 13a). During nighttime, the power in 5–10 mHz band is significantly less compared to that during daytime. Nighttime powers in 5–10 mHz and 10–15 mHz frequency bands are comparable (Figure 13b). Power in 15–25 mHz band is found to be very small during both daytime and nighttime. These observations indicate the dominance of larger wavelengths in the quiet time magnetic field measurements at CHAMP during daytime, which reduces significantly during nighttime. As the polar orbiting satellite traverses, it monitors various ionospheric currents present at different latitudes [Jadhav *et al.*, 2002] and hence the spatial frequencies due to equatorial, low- to middle-latitude ionospheric current systems (such as equatorial electrojet (EEJ), Sq , and return flows of EEJ currents) can be present in the magnetic field measurements during daytime. The observations also show that although less, a significant power is present in 10–15 mHz band that is consistently present in both daytime and nighttime, which do not have obvious explanation. Thus, one can realize that significant power in 5–10 mHz and 10–15 mHz frequency bands present on quiet days during daytime could be because of various encompassing ionospheric current systems monitored by CHAMP due to its orbital motion. As a result, the Pi2 oscillations (which are relatively

smaller in amplitude) in the satellite observations may get masqueraded by the spatial frequencies (larger amplitudes) present in the satellite data, especially during daytime.

5. Discussion

Pi2s which are associated with substorm occurrence in the nightside of the magnetosphere are often observed in daytime ground stations simultaneously with their night counterparts [Sutcliffe and Yumoto, 1991]. But their identification in space is mainly limited to nighttime till date. As mentioned in section 1, there are contradicting reports about the identification of daytime Pi2s in LEO satellites and therefore it is puzzling whether to believe or not the existence of daytime Pi2s at topside ionosphere. The main focus of this paper is to examine whether daytime Pi2s identified at ground stations exist simultaneously at topside ionosphere. If yes, how are these waves manifested in CHAMP observations? Does its detection at satellite depend on the frequency of Pi2 oscillation? Bearing these questions in mind, we grouped the Pi2s on the basis of its characteristic frequencies into three subgroups (6–10 mHz, 10–15 mHz, and 15–25 mHz).

Although polar LEO satellites provide an opportunity to look into Pi2 oscillations at topside ionosphere, it can impose certain limitations in monitoring these waves. One of the important limitations which may affect these oscillations is the Doppler effect that arises due to the motion of satellite. As Pi2 oscillations at low to middle latitudes are considered to be primarily compressional, we consider the source speed as Alfvén speed ($v_{\text{Alfvén}}$), which is the lower limit of the speed with which compressional waves travel and the receiver speed as speed of CHAMP satellite (v_{Sat}), which is computed to be 7.7 Km/s. Frequency observed by satellite (f_{Sat}) due to its motion is given by equation (1), where f_0 is the actual frequency of the waves. In the inner magnetosphere during daytime the typical Alfvén speed is ~ 200 Km/s, which gives $f_{\text{Sat}} \approx f_0$, as $\frac{v_{\text{Sat}}}{v_{\text{Alfvén}}}$ is much less than unity. The percentage change in the observed frequency is computed to be less than 4% of the actual frequency. Hence, one can conclude that the Doppler effect due to motion of the satellite is very small for the compressional component of Pi2 oscillations observed by CHAMP.

$$f_{\text{Sat}} = f_0 \left[1 + \frac{v_{\text{Sat}}}{v_{\text{Alfvén}}} \right] \quad (1)$$

All the daytime Pi2 events identified in the present study are first examined at day and night ground stations for highly coherent (coherence >0.8) and in-phase oscillations with matching waveforms, confirming the global occurrence of the Pi2. The amplitude of the Pi2s at daytime ground station is found to be much smaller than nighttime ones. Although daytime Pi2s are identified at ground, their identification at satellite is not straightforward. The identification of daytime Pi2s at satellite depends strongly on the characteristic frequency of Pi2. It is relatively difficult to identify the coherent frequencies in the lower end of the frequency range of Pi2, while the Pi2s occurring at the higher end of the range are mostly coherent with underneath ground observations. This is because of the existence of background (non-Pi2) lower frequencies present at satellite during daytime. The general characteristics of daytime Pi2s observed in the present study such as smaller-amplitude and out-of-phase oscillations at CHAMP compared to underneath ground observations are in accordance with the findings by Han *et al.* [2004]. Daytime observations of low-latitude Pi2s on ground were explained by invoking instantaneous penetration of electric field variations from polar to dayside equatorial to low-latitude ionosphere, where electric currents associated with this penetrated electric field would produce Pi2 oscillations in the magnetic field on the ground [Kikuchi and Araki, 1979; Shinohara *et al.* [1997]; Yumoto and CPMN group, 2001, and references therein]. Similar explanation for the daytime Pi2 observed in Ørsted data was quoted by Han *et al.* [2004]. They attributed the lower amplitude at satellite to longer distance of Ørsted (>500 km) from the ionospheric current height (~ 110 km) and also to the induced currents in the Earth surface. However, Sutcliffe and Lühr [2010] found no coherent Pi2 oscillations in CHAMP, which they explained with the same penetration model of Kikuchi and Araki [1979], but with the assumption that the model is homogeneous in the east-west direction. Under this assumption, the magnetic field due to ionospheric current is confined between the ionosphere and the ground [Kikuchi and Araki, 1979] and therefore magnetic field oscillations of Pi2s cannot be observed above the ionosphere. They also mentioned the effect of Earth-induced current (similar to Han *et al.* [2004]) in nullifying the Pi2 signature above the ionosphere. However, the above mentioned assumption is not valid in the actual scenario of the ionospheric currents, and hence, it is possible to get magnetic field variations above the ionosphere with opposite direction to that on ground. Thus, our daytime Pi2 observations can also be

explained by the existing understanding. However, the cited penetration model of *Kikuchi and Araki* [1979] is considered to be questionable [*Yumoto et al.*, 1997].

The important question is why the measurements from the same satellite are revealing two different conclusions (present paper and *Sutcliffe and Lühr* [2010]). Also, why could *Han et al.* [2004] identify only two cases of daytime Pi2s in the Ørsted data, whereas majority of the Pi2 events showed poor correlation between Ørsted and ground observations? Present analysis focusing on different bins within Pi2 frequency band can provide answer to these questions. Normally, Pi2 oscillations are more likely to occur in the lower side of the conventional Pi2 band as evident from ground observations [*Li et al.*, 2000]. Our analysis shows that these oscillations are more prone to contamination at satellite height during daytime, and only very intense events will be observed simultaneously at satellite and ground. This is why *Sutcliffe and Lühr* [2010] could not identify daytime Pi2 in CHAMP data and *Han et al.* [2004] were able to observe limited number of daytime events at satellite.

Another issue raised by *Sutcliffe and Lühr* [2010] is about the nonuniformity in the observation of out-of-phase oscillations between Ørsted and ground, as they noticed four daytime cases in the reports of *Han et al.* [2004], with $CC > 0.6$ but with in-phase oscillations. It should be noted that these events occurred when the satellite was either in the morning or evening sector and mostly confined to the latitudinal range 20° – 60° . It is possible that during these events, the ionospheric conductivity was smaller and the penetrated electric fields may not have significant role to play. Therefore, the in-phase oscillations at satellite and ground could be thought of as result of cavity oscillations whose dominance was significant compared to penetrated fields.

According to the present understanding, the Pi2s observed at any location on ground or space mainly comprises of contributions from a substorm current wedge oscillations, inner magnetospheric cavity-like oscillations, a surface wave at the plasmopause, a bouncing mode of impulsive field-aligned currents at auroral latitudes, and penetration of Pi2 electric field from auroral latitude to the dayside equatorial ionosphere [*Olson*, 1999; *Yumoto and CPMN group*, 2001]. For low- to middle-latitude Pi2s, essentially two components, viz., cavity-mode oscillations and an instantaneous transmission of electric field from high- to low-latitude ionosphere, are responsible. For nightside low-latitude Pi2, the earlier one is dominant, while for Pi2s at the terminator to dayside, both the sources contribute. The effect of the penetration of Pi2 electric field mainly depends on the ionospheric conductivity, so its dominance varies with local time; e.g., near dawn or dusk terminators ionospheric conductivity is relatively weak and hence cavity-mode oscillations are mainly responsible for Pi2 observation, whereas near local noon, ionospheric currents associated with penetrated electric field would play significant role resulting in out-of-phase oscillations between ground and satellite and satellite-to-ground amplitude ratios smaller than unity. At the same time, one cannot rule out the existence of cavity oscillation at dayside, which can give in-phase oscillations above and below the ionosphere.

6. Summary

The present study clearly demonstrates that it is possible to observe daytime Pi2s above the ionosphere. Our findings based on the compressional component at CHAMP and H component at underneath ground station are summarized as follows:

1. During nighttime coherent in-phase oscillations having similar waveform are observed in CHAMP and ground irrespective of whether characteristic Pi2 frequency resides in the lower or higher end of Pi2 band.
2. Mostly, the amplitude of nighttime Pi2s is found to be comparable or slightly greater at satellite than on the ground.
3. Around 90% of the nighttime events showed Pi2 signatures in the poloidal component as well, thereby confirming the cavity-mode resonance as viable generation mechanism for nighttime Pi2 oscillations.
4. Although daytime Pi2s are observed on ground, their identification at satellite is not straightforward.
5. Detection of daytime Pi2s at satellite depends on its characteristic frequency.
6. During daytime, Pi2s with higher frequencies (>15 mHz) can be considered more suitable for the detection in the topside ionosphere using polar LEO satellites, provided that suitable band pass filter avoiding background frequencies at satellite is applied.
7. The satellite to ground amplitude ratio is found to be dependent on the characteristic Pi2 frequency. In general, the satellite to ground amplitude ratio is found to be less than 1 during daytime.

8. During noon time, Pi2 oscillations at satellite are out of phase with respect to those observed on the ground.
9. The inability of earlier studies to detect Pi2s in polar LEO satellites could be due to significant modulation of Pi2s by the background non-Pi2 frequencies present in daytime satellite passes.
10. It is proposed that a combination of fast cavity-mode oscillations and an instantaneous transmission of Pi2 electric field from high- to low-latitude ionosphere is the responsible mechanism for the daytime Pi2 oscillations. The relative dominance of these two processes is determined by prevailing ionospheric conductivity. Higher ionospheric conductivity would result in the dominant effect of penetration electric fields from high to low latitude, whereas cavity-mode oscillation would prevail during low-conductivity state of the ionosphere.

Acknowledgments

The authors are thankful to Information System and Data Center (ISDC) for providing high-quality 1 s vector magnetic field data from CHAMP satellite. The data are available on request from ISDC at <http://isdc.gfz-potsdam.de/>, data set name: CH-ME-2-FGM-NEC. We also thank WDC for Geomagnetism, Kyoto (<http://wdc.kugi.kyotou.ac.jp/caplot/index.html>), USGS (<http://cda-web.gsfc.nasa.gov/cgi-bin/eval1.cgi>), and British Geological Survey for making available 1 s data from ground observatories. Data from KAK, TFS at WDC, Kyoto, and SJG, BSL, HON at CDAWeb are freely available at the respective links. Ground data from ASC magnetic observatory were obtained on request.

Larry Kepko thanks Viacheslav Pilipenko and one anonymous reviewer for their assistance in evaluating this paper.

References

- Cuturrufo, F., V. Pilipenko, B. Heilig, M. Stepanova, H. Lühr, P. Vega, and A. Yoshikawa (2014), Near-equatorial Pi2 and Pc3 waves observed by CHAMP and SAMBA/MAGDAS stations, *Adv. Space Res.*, *55*, 1180–1189, doi:10.1016/j.asr.2014.11.010.
- Han, D.-S., T. Iyemori, M. Nose, H. McCreadie, Y. Gao, F. Yang, S. Yamashita, and P. Stauning (2004), A comparative analysis of low-latitude Pi2 pulsations observed by Ørsted and ground stations, *J. Geophys. Res.*, *109*, A10209, doi:10.1029/2004JA010576.
- Jadhav, G., M. Rajaram, and R. Rajaram (2002), A detailed study of equatorial electrojet phenomenon using Ørsted satellite observations, *J. Geophys. Res.*, *107*(8), 1175, doi:10.1029/2001JA000183.
- Keiling, A., and K. Takahashi (2011), Review of Pi2 models, *Space Sci. Rev.*, *161*, 63–148, doi:10.1007/s11214-011-9818-4.
- Kikuchi, T., and T. Araki (1979), Horizontal transmission of the polar electric field to the equator, *J. Atmos. Terr. Phys.*, *41*, 927–936.
- Kim, K.-H., H.-J. Kwon, D.-H. Lee, H. Jin, K. Takahashi, V. Angelopoulos, J. W. Bonnell, K. H. Glassmeier, Y.-D. Park, and P. Sutcliffe (2010), A comparison of THEMIS Pi2 observations near the dawn and dusk sectors in the inner magnetosphere, *J. Geophys. Res.*, *115*, A12226, doi:10.1029/2010JA016010.
- Li, Y., K. Yumoto, and the 210 MM Magnetic Observation Group (2000), Local time dependence of Pi2 pulsations observed along the 210 magnetic meridian, *Mem. Fac. Sci., Kyushu Univ.*, *31*(1), 11–18.
- Maus, S., and H. Lühr (2005), Signature of the quiet-time magnetospheric magnetic field and its electromagnetic induction in the rotating Earth, *Geophys. J. Int.*, *162*, 755–763.
- Nishimura, Y., L. R. Lyons, T. Kikuchi, V. Angelopoulos, E. Donovan, S. Mende, P. J. Chi, and T. Nagatsuma (2012), Formation of substorm Pi2: A coherent response to auroral streamers and currents, *J. Geophys. Res.*, *117*, A09218, doi:10.1029/2012JA017889.
- Nose, M., et al. (2003), Multipoint observations of a Pi2 pulsation on morningside: The 20 September 1995 event, *J. Geophys. Res.*, *108*(A5), 1219, doi:10.1029/2002JA009747.
- Nose, M., K. Liou, and P. R. Sutcliffe (2006), Longitudinal dependence of characteristics of low-latitude Pi2 pulsations observed at Kakioka and Hermanus, *Earth Planets Space*, *58*, 775–783.
- Nose, M., et al. (2009), New substorm index derived from high-resolution geomagnetic field data at low latitude and its comparison with AE and ASY indices, in *Proceedings of XIIIth IAGA Workshop on Geomagnetic Observatory Instruments, Data Acquisition, and Processing*, U.S. Geol. Surv. Open File Rep., vol. 2009–1226, pp. 202–207, U.S. Geol. Surv., Reston, Va.
- Nose, M., et al. (2012), Wp index: A new substorm index derived from high-resolution geomagnetic field data at low latitude, *Space Weather*, *10*, S08002, doi:10.1029/2012SW000785.
- Olson, J. V. (1999), Pi2 pulsations and substorm onsets: A review, *J. Geophys. Res.*, *104*, 17,499–17,520, doi:10.1029/1999JA900086.
- Rajaram, R., J. M. Ruohoniemi, R. A. Greenwald, and K. B. Baker (1992), A new method for detecting the projection of magnetospheric oscillations into the ionosphere, *J. Geophys. Res.*, *97*, 16,959–16,969, doi:10.1029/92JA00830.
- Sakurai, T., and T. Saito (1976), Magnetic pulsation Pi2 and substorm onset, *Planet. Space Sci.*, *24*, 573–575.
- Sastry, T. S., Y. S. Sarma, S. V. S. Sarma, and P. V. Sanker-Narayan (1983), Day-time Pi2 pulsations at equatorial latitudes, *J. Atmos. Terr. Phys.*, *45*, 733–741.
- Shinohara, M., K. Yumoto, A. Yoshikawa, O. Saka, S. I. Solov'ev, E. F. Vershinin, N. B. Trivedi, J. M. Da Costa, and The 210 MM Magnetic Observation Group (1997), Wave characteristics of daytime and nighttime Pi2 pulsations at the equatorial and low latitudes, *Geophys. Res. Lett.*, *24*, 2279–2282, doi:10.1029/97GL02146.
- Stuart, W. F., and H. G. Barcszus (1980), Pi's observed in the daylight hemisphere at low latitudes, *J. Atmos. Terr. Phys.*, *42*, 487–497.
- Sutcliffe, P. R., and H. Lühr (2003), A comparison of Pi2 pulsations observed by CHAMP in low Earth orbit and on the ground at low latitudes, *Geophys. Res. Lett.*, *30*(21), 2105, doi:10.1029/2003GL018270.
- Sutcliffe, P. R., and H. Lühr (2010), A search for dayside Pi2 geomagnetic pulsations in the CHAMP low-Earth-orbit data, *J. Geophys. Res.*, *115*, A05205, doi:10.1029/2009JA014757.
- Sutcliffe, P. R., and K. Yumoto (1989), Dayside Pi2 pulsations at low latitudes, *Geophys. Res. Lett.*, *16*, 887–890, doi:10.1029/GL016i008p00887.
- Sutcliffe, P. R., and K. Yumoto (1991), On the cavity mode nature of low-latitude Pi2 pulsations, *J. Geophys. Res.*, *96*, 1543–1551, doi:10.1029/90JA02007.
- Takahashi, K., S. I. Ohtani, and B. J. Anderson (1995), Statistical analysis of Pi2 pulsation observed by the AMPTE CCE spacecraft in the inner magnetosphere, *J. Geophys. Res.*, *100*, 21,929–21,941, doi:10.1029/95JA01849.
- Takahashi, K., B. J. Anderson, and K. Yumoto (1999), Upper Atmosphere Research Satellite observation of a Pi2 pulsation, *J. Geophys. Res.*, *104*, 25,035–25,045, doi:10.1029/1999JA900317.
- Yanagihara, K., and N. Shimizu (1966), Equatorial enhancement of micropulsation Pi2, *Mem. Kakioka Magn. Obs.*, *12*, 57–63.
- Yumoto, K. (1986), Generation and propagation mechanisms of low-latitude magnetic pulsations—A review, *J. Geophys. Res.*, *60*, 79–105.
- Yumoto, K., and CPMN group (2001), Characteristics of Pi2 magnetic pulsations observed at the CPMN stations: A review of the STEP results, *Earth Planets Space*, *53*, 981–992.
- Yumoto, K., V. Pilipenko, E. Fedorov, N. Kurneva, and M. De Lauretis (1997), Magnetospheric ULF wave phenomena stimulated by SSC, *J. Geomag. Geoelectr.*, *49*, 1179–1195.